Available online at www.sciencedirect.com

ScienceDirect

Physics Procedia 62 (2015) 84 – 91

Physics Procedia

3rd International Conference Frontiers in Diagnostic Technologies, ICFDT3 2013

X-ray High-Resolution Spectroscopy for Laser-Produced Plasma

F. Barbato[b], D. Scarpellini[b], A. Malizia[b], P. Gaudio[b], M. Richetta[b], L. Antonelli[a,b]

[a] *Université Bordeaux, CNRS, CEA, CELIA (Centre Lasers Intenses et Applications), UMR 5107, F-33405 Talence, France*
[b] *Dipartimento di Ingegneria Industriale, Università degli Studi di Roma "Tor Vergata", Via del Politecnico 1, 00133-Rome, Italy*

Abstract

The study of the emission spectrum gives information about the material generating the spectrum itself and the condition in which this is generated. The wavelength spectra lines are linked to the specific element and plasma conditions (electron temperature, density), while their shape is influenced by several physical effects like Stark and Doppler ones.
In this work we study the X-ray emission spectra of a copper laser-produced plasma by using a spherical bent crystal spectrometer to measure the electron temperature. The facility used is the laser TVLPS, at the Tor Vergata University in Rome. It consists of a Nd:Glass source (in first harmonic - 1064 nm) whose pulse parameters are: 8 J in energy, time duration of 15 ns and a focal spot diameter of 200 μm. The adopted spectrometer is based on a spherical bent crystal of muscovite. The device combines the focusing property of a spherical mirror with the Bragg's law. This allows to obtain a great power resolution but a limited range of analysis. In our case the resolution is on average 80 eV. As it is well-known, the position of the detector on the Rowland's circle is linked to the specific spectral range which has been studied. To select the area to be investigated, we acquired spectra by means of a flat spectrometer. The selected area is centered on 8.88 Å. To calibrate the spectrum we wrote a ray-tracing MATLAB code, which calculates the detector alignment parameters and calibration curve. We used the method of line ratio to measure the electron temperature. This is possible because we assumed the plasma to be in LTE condition. The temperature value was obtained comparing the experimental one, given by the line ratio, with the theoretical one, preceded by FLYCHK simulations.

Peer-review under responsibility of the ENEA Fusion Technical Unit
Keywords: X-ray spectroscopy, laser-plasma, spherical bent crystal ;

1. Introduction

The study of the X-ray emission of plasma has an important role in physics. From the atomic point of view we can acquire information about the atomic structure of the atom shells. Moreover, X-ray emissions from plasma are useful to understand plasma conditions like electronic temperature and density. This is interesting to understand astrophysical plasmas, but also, in laboratory-produced plasmas. Several effects occur in laser-produced plasma at different laser intensities. At low laser intensities the study of optical emissions can provide useful information about the physical conditions (Laser Induce Breakdown Spectroscopy). At higher intensities back-ground temperature increases and

E-mail address: francescobarbato.mail@gmail.com

Peer-review under responsibility of the ENEA Fusion Technical Unit
doi:10.1016/j.phpro.2015.02.015

soft X-ray emission spectrum of the material provides information about temperature and density. The interaction of high electromagnetic field can accelerate charged particles like electrons. In this case suprathermal electrons can collides with the inner shell of the atoms and the result is Kα radiation emission from solid material. Kα radiation is crucial to study the propagation of suprathermal electrons in matter for many fields, like the Inertial Confinement Fusion (*Šmíd* et al. (2013); Antonelli et al. (2011)). Moreover in laser-produced plasma the typical density is similar to the solid density or higher. In this conditions Stark effect becomes important, influencing the emitted line shape. The presence of strong magnetic fields can have, as result Zeeman effect spitting the emission lines. Furthermore the high velocities of the ion in the expanding plasma corona produce a Doppler shift. X-ray spectroscopy acquires an important role to study all these effects. Different techniques were developed in this fields. In this work we present a particular spectrometer based on a spherically bent crystal. Its particularity is the combination of the properties of Bragg's diffraction and spherical mirror. The result is depicted as a 2D image, with energy resolution in one axis and spatial resolution in the other one.

2. Plasma models

The interaction of the laser light at a certain intensity ionizes the material. Two conditions must be satisfied to generate ions with ionization potential E_i in a plasma:

$$T_e \gtrsim \eta E_1 \tag{1}$$

where T_e is the electron temperature of the plasma and $\eta \simeq 0.1$ for LTE, while $\eta = 0.2$ for corona equilibrium (Vainshtein et al., 1979). The second condition is:

$$\Delta t \gtrsim \delta t_i \tag{2}$$

where Δ_t is the lifetime of the plasma and $\delta t_i = [N_e < v\ sigma_i >]^{-1}$ is the ionization time for the given ions, N_e is the electron density and $< v\sigma_i >$ is the rate of ionization by electron impact.
The energy of the laser beam photons is low, so the efficiency of the direct ionization of the matter is low. Ionization is the result of the collision between the electron and the atom with the absorption of a photon. This mechanism is possible only if there are free electrons in the point where the laser hit the matter. This process is called collissional absorption. The plasma created by the interaction start to expand in normal and opposite direction with respect to the surface of the target. The ablation pressure generate an inward shockwave in the material. At high laser energy and intensity the shockwave can achieve pressures in the order of Mbar. This is the base of the idea of the ICF. This kind of pressure were characterized in many experiment related to the study of the equation of state of many material for astrophysical interest and for fusion science. X-ray comes out from the interaction region between laser and target. For a given laser wavelength the specific density, where the wave vector becomes zero, is called critical density and it is given by:

$$n_c = \frac{1.11 \times 10^{21}}{\lambda_0^2} cm^{-3} \tag{3}$$

where λ_0 is the wavelength of the laser in μm. In general the soft X-ray emission from a laser-produced plasma comes from this specific region. The level population distribution of atoms in a plasma is closely related to thermodynamic parameters such as plasma temperature and density. So this is important in the analysis of plasma spectra in order to quantify internal parameters like energy, density (electronic and ionic) and opacity.
To describe the relation between these plasma parameters and the population kinetic exist different theoretical models according to different thermodynamic conditions.

2.1. Local Thermodynamic Equilibrium

The Local Thermodynamic Equilibrium (LTE) model describes a plasma state where each atomic process are in *detailed balance*. This means that the rate of every atomic process (except the radiation process) are perfectly balanced

by their inverse process.
The density population of level i in atom with ionization degree z with temperature T is described by the Boltzmann distribution:

$$n_{iz} = \frac{N_z}{U_z(T)} g_{iz} exp\left(-\frac{E_{iz}}{kT}\right) \tag{4}$$

where N_z is the total number of ions z, g_{iz} is the statistical weight assigned to the level i of ion z, E_{iz} is the excitation energy relative to the ground state, U_z is the partition function of ion z.
The ground level population of ion z is related to the ground level population of ion z+1 by the Saha ionization equation:

$$n_{0,z} = \frac{n_{0,z+1} n_e}{2} \frac{g_{0,z}}{g_{0,z+1}} \left(\frac{h^2}{2\pi m_e kT}\right)^{3/2} exp\left(\frac{E_{Iz}}{kT}\right) \tag{5}$$

The free electrons have a Maxwellian energy distribution as in the TE case. The radiation field in LTE plasmas however, is no longer a Planck function and it depends not only on local plasma conditions but also on population distributions and atomic transition probabilities.
The LTE state is often found in plasma laboratory, where the relatively high density and low temperature allow the collisional process to dominate over the radiative process.
Even in non-LTE plasmas, it is always possible to find levels for which collisional transitions are highly favored over radiative transitions depending on plasma conditions. Those levels are still said to be in partial LTE and such plasmas are said to be partial LTE plasmas. The Boltzmann and Saha equations can be conveniently applied for the relative population distributions among the levels in partial LTE.

2.2. Spectral Intensity Analysis

Radiation emitted from the radiation field in a plasma can originate from three types of radiative transitions: bound-bound transitions, bound-free transitions and free-free transitions.
Line radiation emitted from a bound-bound transition has a peak intensity at a frequency corresponding to the energy difference between two bound levels.
Bound-free transitions is a recombination radiation whose radiation frequency corresponds to the sum of the kinetic energy of the recombining electron and the binding energy of the shell that the electron falls to. Recombination radiation has a discontinuity at the frequency corresponding to the binding energy and it is distributed over higher frequencies starting at the threshold frequency.
Bremsstrahlung radiation is emitted from free-free transitions when a free electron loses its kinetic energy in a collision with electrons and ions. The emitted radiation frequency corresponding to the change in electron kinetic energy, is distributed continuously over all frequencies. Recombination radiation and Bremsstrahlung radiation are called continuum radiation since their intensities are distributed over a wide range of frequency unlike line radiation whose intensity is peaked at a line-center frequency.
A common method in interpreting measured spectra is to use a ratio of line intensities in determining electron temperature and density. If a plasma is optically thin, for a line radiation from level j to level i, the intensity which is integrated along the line of sight s, can be written as:

$$I_{ji} = \frac{1}{4\pi} \int n_j A_{ji} h\nu_{ji}\, ds \tag{6}$$

where A_{ji} is an atomic transition probability of level j to i and $h\nu_{ji}$ is an energy of the emitted photon. The quantity n_j is the upper level population density. The ratio of two line intensities is commonly used if relative population density is known as a function of plasma parameters:

$$\frac{I_1}{I_2} = \frac{n_1 A_1 h\nu_1}{n_2 A_2 h\nu_2} \tag{7}$$

where n_1 and n_2 are the upper levels of line radiation and $h\nu_1$ and $h\nu_2$ are radiation frequencies. If the two upper levels are in local thermodynamic equilibrium (LTE), the relative population is solely a function of electron temperature. Using the Boltzmann relation 4, the ratio of two line intensities is written as:

$$\frac{I_1}{I_2} = \frac{g_1 A_1 h\nu_1}{g_2 A_2 h\nu_2} exp\left[-\frac{E_1 - E_2}{kT_e}\right] \tag{8}$$

where g_1 and g_2 are statistical weights of level 1 and 2. E_1 and E_2 are the energies of level 1 and 2. By taking logarithms in both sides,

$$\log\left[\frac{I_1}{g_1 A_1 h\nu_1}\right] - \log\left[\frac{I_2}{g_2 A_2 h\nu_2}\right] = -\frac{E_1 - E_2}{kT_e} \tag{9}$$

By means of several measured line intensities, a plot is constructed with data points (x,y) using the quantity, a logarithmic value of a line intensity divided by its ($gAh\nu$) as y component and the energy of the upper level as x component. If the data points are fitted in a straight line, the gradient will be a negative value of the inverse of electron temperature. This plot is called Boltzmann plot. In this analysis, it is important to choose lines in such a way that the energy differences of the upper levels are comparable to or larger than electron temperatures. Otherwise, the ratio is insensitive to electron temperature.

3. Experimental Setup

The plasma was generated by a Nd:Glass laser. It is a table top laser system with four amplifiers TLPS (Francucci et al. (2011)).
The interaction occurred inside a vacuum chamber ($10^{-2} mbar$). The laser beam hit the target (copper) with an incident angle of 45°
The spherically bent crystal spectrometer was placed inside the vaccum chamber. As detector we used a X-ray film *KODAK RAR 2492*. The film was screen by a double layer of aluminum ($0.2\mu m$) and mylar ($1\mu m$). This filters were necessary to prevent the film to the direct exposure of visible and UV light.
To select the range of work of our focusing spectrometer we also used a flat crystal spectrometer which has a worse resolution but a wider range. The crystal was a RbHP (Rubidium Hydrogen Phthalate) with lattice spacing $2d = 26.12$ *Å* Mattoccia (2011).
We recorded the emission spectra from the L-shell of Copper according what we expected to see due to the characteristic of our laser system.

4. Spherical Bent Crystal Spectrometer

The spectrometer used is a FSSR-JG-100 provide by the Multicharged Ions Spectra Data Center of VNIIFTRI Institute (Moscow, Russia) (tab. 1). The peculiarity is a spherically bent crystal of mica (muscovite). It combines the focusing property of a spherical mirror with the Bragg's diffraction of a crystal described by (Faenov et al. (1994); Pikuz et al. (2004); Hölzer et al. (1998)):

$$2d \sin\theta = n\lambda \tag{10}$$

d is the lattice spacing, λ the wavelength of the incoming light, θ the Bragg's angle and n is the diffraction order.

This allows to increase the transmission coefficient of the spectrometer with high spatial resolution. The arrangement of the instruments is depicted in fig. 1. The spectral focusing is the same as that in the Johann's spectrometer Johann (1931), but in this case the crystal is bent around a cylindrical surface. The difference is the possibility to focus in a direction perpendicular to the dispersion direction (in the sagittal plane).

Let us consider a spherically crystal of radius R_c (2) and a source S that emits monochromatic radiation of wavelength λ. Because of the dispersive properties of the crystal the radiation will only be reflected if it has passed trough a point O lying on the Rowland's circle ($R = R_c \setminus 2$). After being reflected from the crystal, the radiation will be focused at a point O' conjugate with O. A one-to-one relationship exists between the point of the Rowland's circle

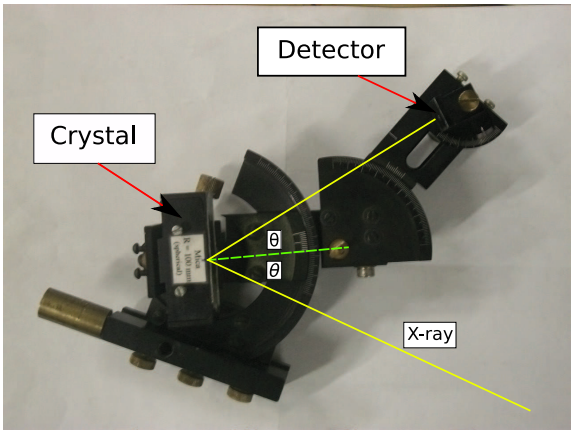

Fig. 1.

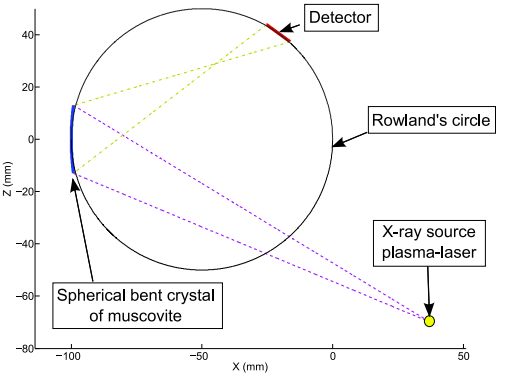

Fig. 2. Scheme of working of a spherical crystal in spectrometer focusing mode

and the wavelength of the diffracted rays. Thus, by placing a detector tangent to the Rowland's circle only the rays with a specific wavelength, diffracted by the crystal, hit the detector itself.
In order to obtain a 1-D image in focus on the detector the source is placed to a precise distance from the crystal. To evaluate this distance we start from the focusing mirror law:

$$\frac{1}{b} + \frac{1}{a} = \frac{1}{f} \tag{11}$$

b is the distance crystal-detector, given by:

$$b = 2R \sin\theta \tag{12}$$

f is the focal length of the spherically crystal

$$f = \frac{R}{\sin\theta} \tag{13}$$

Substituting the 12 and 13 in the equation 11, than expliciting it for a we obtain

$$a = \left| \frac{2R \sin\theta}{\cos(2\theta)} \right| \tag{14}$$

The Bragg's angle θ used in the equation above is the one used to set the spectrometer. This is the complementary angle of the incident one at the center of the crystal. To evaluate the spectral range the equation is the same as for the

Table 1. Specifications of spherically bent mica crystal spectrometer

Spectrometer model	FSSR-JG-100
2d (Muscovite)	19.9149 Å
Crystal curvature radius (R_c)	100 mm
Crystal length (Lc)	26 mm (+2 mm in side the box)
Crystal width (lc)	8 mm (+2 mm inside the box)
Maximum spatial resolution (Δx)	(1020) m (limited by the pixel or film grain sizes)
Spectral resolution	4 mÅ
Spectral range	up to 10 keV
Range of analysis	80 eV

Johann's scheme. In particular the extreme values of wavelength that the device can record are:

$$\frac{\lambda_{min}}{2d} = \cos\left(\alpha - \arctan\frac{2\alpha\cos(\theta-\alpha)}{L-2\alpha\sin(\theta-\alpha)}\right) \tag{15}$$

$$\frac{\lambda_{max}}{2d} = -\cos\left(\alpha + \arctan\frac{2\alpha\cos(\theta+\alpha)}{L-2\alpha\sin(\theta+\alpha)}\right) \tag{16}$$

where $\alpha = \arcsin\frac{4R}{L}$, L is the size of the crystal.
The spatial resolution of a spherical crystal bent is determined by spherical aberration, the width of the reflective curve and the quality of the crystal itself.

5. Energy Calibration

A MATLAB code has been written with the aim to evaluate the energy range of the spectrometer by using crystal dimensions and the Bragg's angle as input data. The same code generates a calibration curve that relates any point of the film with an energy value. This is strictly correlated to the alignment of the detector on the Rowland circle and the alignment of the entire spectrometer with respect to the source. In the fig 3 there are the calibration curves generated from the code. The calibration is linear (blue line) if the surface of the detector is tangent to the Rowland's circle. The other two curves (red lines) the angle between the detector surface and the radius of the Rowland's circle is above and below 90 degree (tangent condition). In this experimental setup it is not possible to control this angle so these curves cannot be used to calibrate the spectrum. However these simulations show that the energy range of the spectrometer, with a fixed Bragg's angle, is the same rotating the detector around the tangent position.
The energy range (1360 - 1440 eV) obtained has been used to perform simulations with FLYCHK code Chung et al. (2008, 2005) in order to identify the transition lines. Line identification is necessary to calibrate in energy the spectrum.

6. Data Analysis

The equation 3 is used to calculate the electron density. Using a laser with a wavelength of $1.064\mu m$ the electron density is 1×10^{21}.
Assuming a plasma in LTE regime it is possible to measure its electronic temperature by the ratio of the intensity lines and compare with FLYCHK simulations.
The transition lines *1s(2) 3s+ - 1s(2) 2p+* (at 9.04 Å), *1s(2) 3d+ - 1s(2) 2p+* (at 8.84 Å) and *1s(2) 3d- - 1s(2) 2p-* (at 8.70 Å) are used to measure the electron temperature. In the picture (4) are depicted the experimental ratios normalized with the theoretical ones calculated for different values of electronic temperature and opacity. The green points are the ratio between the lines 8.70/8.84 Åthe red ones the ratio between 8.70/9.04 Å
. The plot show that the temperature of the plasma is from 270 eV to 280 eV. For these values the two ratios cross close to one.

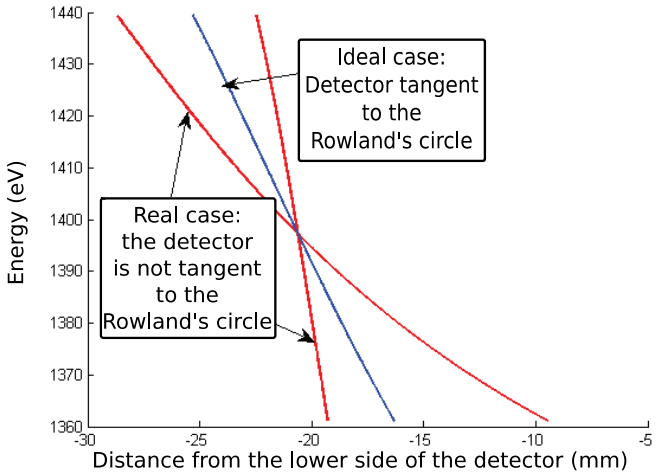

Fig. 3. Calibration curves of the spectrometer obtained from different alignment

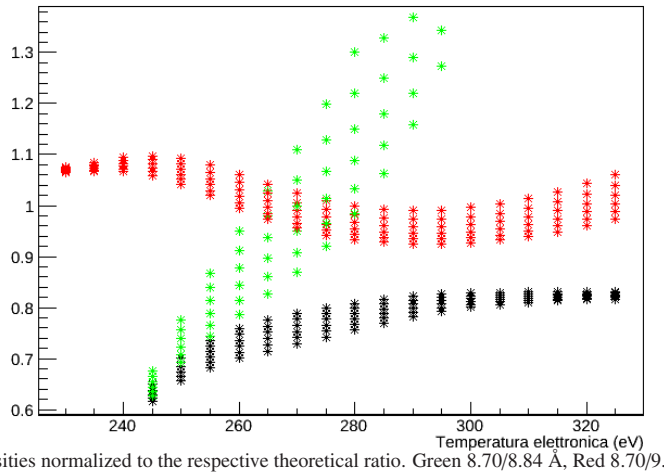

Fig. 4. Ratio of two line intensities normalized to the respective theoretical ratio. Green 8.70/8.84 Å, Red 8.70/9.04 Å, Black χ^2

In picture 5 the simulated spectra with these two values of temperature are superimposed over the experimental one.

7. Conclusion

In this work we use a muscovite crystal in spectrometer mode to measure the electron temperature of plasma micro sources investigations.
In fig. 5 the experimental spectrum and two simulated ones are shown. By using the line ration we found two spectra which have plasma emission condition similar to the experimental one (fig. 4).
These ratios are evaluated for different values of electronic temperature and opacity. The parameters of these simula-

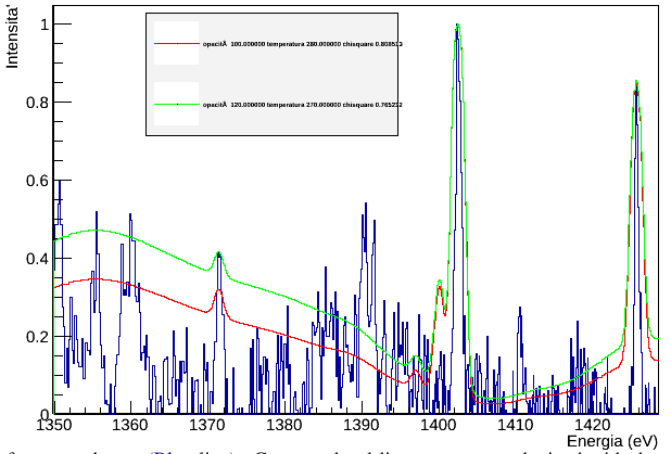

Fig. 5. Experimental X-ray spectra of copper plasma (Blue line). Green and red line are spectra obtained with the code FLYCHK a electron temperature of 270 eV and 0.15 mm as opacity (Green), 280 eV and 0.1 mm (Red)

tions are 270 and 280 eV as electronic temperature, with an opacity respectively of 0.15 and 0.10 mm. The 270 eV simulated spectrum is the best approximation to the experimental data.
The uncertainty is due to several factors. The alignment of the spectrometer to the X-ray source (the plasma) and the position of the detector on the Rowland's circle. The displacement of the device (crystal plus detector) is important to have a spectrum in focus and homogeneous instrumental line broadening over the entire spectrum.
The not perfect agreement with experimental and theoretical data is due to the simulator itself. FLYCHK give a best approximation for H-like and He-like atoms, in this case there is a Li-like Copper ions. The extreme spectral resolution power of this device allows to record the broadening of spectral line in order to make a possible evaluation of the temperature and density of ions distributions.

References

Antonelli, L., Batani, D., Patria, A., Ciricosta, O., Cecchetti, C.A., Koester, P., Labate, L., Giulietti, A., Gizzi, L.A., Moretti, A., et al., 2011. Laserplasma coupling in the shock-ignition intensity regime. Acta technica ČSAV 56.

Šmíd, M., Antonelli, L., Renner, O., 2013. X-ray Spectroscopic Characterization of Shock-Ignition-Relevant plasmas. Acta Polytechnica 53.

Chung, H.K., Chen, M., Morgan, W., Ralchenko, Y., Lee, R., 2005. Flychk: Generalized population kinetics and spectral model for rapid spectroscopic analysis for all elements. High energy density physics 1, 3–12.

Chung, H.K., Lee, R.W., Chen, M.H., Ralchenko, Y., 2008. The How To For FLYCHK,NIST.

Faenov, A.Y., Pikuz, S.A., Erko, A.I., Bryunetkin, B.A., Dyakin, V.M., Ivanenkov, G.V., Mingaleev, A.R., Pikuz, T.A., Romanova, V.M., Shelkovenko, T.A., 1994. High-performance x-ray spectroscopic devices for plasma microsources investigations. Physica Scripta 50, 333.

Francucci, M., Gaudio, P., Martellucci, S., Richetta, M., 2011. Spectroscopy Methods and Applications of the Tor Vergata Laser-Plasma Facility Driven by GW-Level Laser System. International Journal of Spectroscopy 2011.

Hölzer, G., Wehrhan, O., Förster, E., 1998. Characterization of flat and bent crystals for x-ray spectroscopy and imaging. Crystal Research and Technology 33, 555–567.

Johann, H.H., 1931. Z. Phys. 69.

Mattoccia, A., 2011. Caratterizzazione spettroscopica di plasmi mediante ausilio codice numerico. Master's thesis. Universit di Roma Tor Vergata.

Pikuz, T., Faenov, A., Skobelev, I., Magunov, A., Labate, L., Gizzi, L., Galimberti, M., Zigler, A., Baldacchini, G., Flora, F., et al., 2004. Easy spectrally tunable highly efficient x-ray backlighting schemes based on spherically bent crystals. Laser and Particle Beams 22, 289–300.

Vainshtein, L., Sobelman, I., Iukov, E., 1979. Atomic excitation and spectral line broadening. Moscow Izdatel Nauka 1.